Modeling turbidity currents: the effects of bottom morphology and fluid rheology over the final sediment deposits

Gabriel M. Guerra[1], José J. Camata[2], Paulo Paraizo[3], Adriano M. Cortes[5], Malú Grave[5], Renato Elias[5], Fernando A. Rochinha[4], Álvaro L. G. A. Coutinho[5]

[3]*Department of Mechanical Engineering, Federal Fluminense University Niterói, Brazil gguerra@id.uff.br*
[3]*Computer Sciences Department, Federal University of Juiz de Fora Niterói, Brazil camata@gmail.com*
[3]*Petrobras UO-SEAL Sergipe Operational Unity Aracaju, Sergipe, Brazil paraizo@petrobras.com.br*
[4]*Department of Mechanical Engineering, Federal University of Rio de Janeiro Rio de Janeiro, Brazil faro@mecanica.coppe.ufrj.br*
[5]*cHigh Performance Computing Center and Dept. of Civil Engineering, Federal University of Rio de Janeiro Rio de Janeiro, Brazil calvaro.lga.coutinho@gmail.com*

Abstract. Turbidity currents are the main means by which sediments are transported across the ocean floor and one of the principal mechanisms that leads to the formation of basins hosting oil reservoirs. Detailed modeling of this phenomenon may offer new insights to help geologists to understand the deposition mechanisms and the final stratigraphic form of the reservoir. As turbidity currents propagate over the seafloor, they trigger the evolution of a host of topographical features through the processes of deposition and erosion, such as channels and sediment waves. We aim at enhancing the understanding of the underlying physics, with particular emphasis on the sediment deposition mechanisms. Numerical experiments in setups intended to mimic, partially, as the bed morphology is not allowed to change, close with experimental, have adopted. We present in this work a finite element residual-based variational multiscale formulation applied to the numerical simulation of particle-laden flows. We employ an Eulerian–Eulerian framework to describe the flows in which the mathematical model results from the incompressible Navier–Stokes equation combined with an advection-diffusion transport equation, where viscosity depends non-linearly from the sediment concentration. Sediment-laden turbidity currents interacting with irregular bottoms are investigated. The impact of bed morphology over turbidity currents with viscosity varying with concentration is investigated through quantities of interest such as bottom shear stresses and deposition. The spatial pattern of the deposition and its correlation with flow structures are the main focus of this analysis. Quantitative and qualitative observations of the currents are captured in the experiments, we discuss the morphodynamics of the different scenarios for different bottom bathymetry. Further studies may be carried out in order to constructing new concepts of bedforms generation by density currents.

Keywords: Rheology, Turbidity Currents, HPC

1 Introduction

Gravity currents consist of flows generated from small differences in the local fluid density, often also called density currents, see [1]. The density difference promotes a pressure gradient that drives the flow, for example, this might result from local changes in salinity or temperature. Moreover, it can also be due to the presence of sediment particles in suspension, what motivates the resulting currents to be known as particle-laden or particle-driven flows. Indeed, gravity currents are present in many different contexts and occur naturally as well as caused by human actions, see [2]. Natural examples are avalanches, deep water turbidity currents and volcanic eruptions. On the other hand, industrial accidents can cause dispersion of heavy gases in the atmosphere that propagates through a forehead. A comprehensive list of examples may be found in [1], [3] and [2]. The particles can be carried out for long distances and,

eventually, they will settle, being responsible for sediment deposits generating geological formations of considerable interest for the oil and gas industry. Sedimentation and erosion promoted by particle-laden flows can mold the seabed producing different geological structures such as canyons, dunes, and ripples. Particle-laden flows, many times referred to turbidity currents within the geological community, are the main focus here. They typically develop strong turbulence, which impacts directly the particles ability to move relative to the carrying fluid, to settle or to be re-entrained. Data recorded for turbidity currents in the ocean suggests Reynolds numbers of the order of 10^9 [2]. Depending on what prevails, settling or resuspension, the current, and its turbulent structures might evolve in an entirely different manner, and consequently, those flow changes affect the transport of particles. The spread of a gravity current depends on the boundary conditions, and two cases are usually distinguished based on whether the initial release is of the same width as the environment or not.

In this sense two numerical setups, contemplating these conditions will be studied, inspired in sophisticated laboratory tests, are used for the analysis. A channel or corridor flow with a sustained current is adopted with two bottom configurations. Our findings suggest how turbulent structures and sediment deposition are affected by a particular empirical rheological law interacting with sea floor. The remainder of this paper is organized as follows. In Section 2 we introduce the governing and closure equations. Section 3 presents the computational implementation of the finite element formulation and turbulence modeling adopted. and in Section 4 we show the computational results. The paper ends with a summary of our most important findings.

2 Physical Modeling: phenomenological equations

In this section we present, under an Eulerian-Eulerian framework, the governing equations for turbidity currents developed combining mass and momentum balances with rheological phenomenological models. Through these currents, a mixture of sediments, encompassing different particle sizes, can be carried and eventually deposited on the sea bottom. Sediments are modeled as a continuum and described by the volumetric concentration. As there are no sharp limits of the volumetric sediment concentration defining dilute and nondilute flows, we invoke here the Boussinesq's hypothesis, typically used for the dilute case, but assuming rheological relations that accommodate higher sediment concentrations. Assuming Boussinesq's hypothesis, we intend to propose an extension of the model presented in [] capable of describing nondilute currents. The determination of its domain of validity is outside the scope of the present work, and here we aim at enhancing the understanding of the underlying physics, with particular emphasis on the sediment deposition mechanisms.

2.1 Incompressible flow coupled with particles transport

The spatial domain in which the flow takes place along the time interval $[0, t_f]$ is denoted by $\Omega \subset \mathbb{R}^{n_{dim}}$, where n_{dim} is the number of spatial dimensions, and Γ the boundary of Ω. A velocity-pressure non-conservative form of the Navier-Stokes (NS) equations describes the incompressible turbulent fluid flows carrying suspensions of sediments. We assume that for the scenarios analyzed, particles inertia and particle-particle interactions can be considered negligible. Moreover, we also apply the Boussinesq hypothesis which accounts for the fluid - particle interaction using a forcing term proportional to the local difference in the fluid density due to the presence of sediments. Fluid motion drives the sediment particles, but they are also endowed with extra mobility modeled by their settling velocity u_S, related to grain size sediment in the gravity direction, $\mathbf{e}^g$, uncoupled advection-diffusion equations model the sediment transport. The motion of each grain size, embedded in the mixture, is mapped to the fields $c = C/C_0$ the scaled concentrations, expressing the volume fraction occupied by each particle size. C and C_0 are, respectively, the actual concentration and the initial reference concentration or normalization value, see [4], the latter typically taken as the total initial volume fraction of the particles. Diffusion of the sediment is supposed to be quite small. Motivation by its inclusion in the modeling is often by numerical reasons [5]. Accordingly, the dimensionless equations that govern the particle-laden flow are:

Fluid: Incompressible Navier Stokes

$$\frac{\partial \mathbf{u}}{\partial \mathbf{t}} + \mathbf{u}\,.\nabla \mathbf{u} = -\nabla p + \frac{2}{\nu_f \sqrt{Gr}} \nabla.(\nu_m(c)\nabla^s \mathbf{u}) + \; c\; \mathbf{e}^g \;\; \text{in} \;\; \Omega \times [0, t_f] \tag{1}$$

$$\nabla \,.\, \mathbf{u} = \mathbf{0} \;\; \text{in} \;\; \Omega \times [0, t_f] \tag{2}$$

Sediment Transport: Advection + Diffusion

$$\frac{\partial c}{\partial t} + (\mathbf{u} + u_S \mathbf{e}^g).\nabla c = \nabla. \left(\frac{1}{Sc\sqrt{Gr}} \nabla c \right) \qquad \text{in} \;\; \Omega \times [0, t_f] \tag{3}$$

where $\mathbf{u}$, p and t are, respectively, non-dimensional velocity, pressure and time. Above, p, many times referred in the literature as the dynamic pressure, results after removing the hydrostatic component of the pressure. The rheological function $\nu_m(c)$ of the volumetric concentration, is the effective dynamic viscosity and u_S the particle settling velocity acting in the direction of gravity $\mathbf{e}^g$. Gr is the Grashoff number that expresses the ratio between buoyancy and viscous effects given by:

$$Gr = \left(\frac{u_b H \rho_f}{\nu_f} \right)^2 \tag{4}$$

with ν_f and ρ_f are, respectively, dynamic viscosity and the fluid density, H is a characteristic length of the flow and the buoyancy velocity;

$$u_b = \sqrt{g H c_0 (\tilde{\rho}_p - \tilde{\rho}_f)/\tilde{\rho}_f}$$

where g stands for the gravity acceleration and $\tilde{\rho}_p$ and $\tilde{\rho}_f$ for, respectively, particles and fluid densities. The Reynolds number is such that $Re = Gr^2$. We assume that the different grains have the same density. A third dimensionless number, resulting from turning the governing equations into a non-dimensional form is the Schmidt number, Sc, giving the ratio between diffusion and viscous effects:

$$Sc = \frac{\nu_f}{\kappa \rho_f} \tag{5}$$

where κ is the diffusion coefficient, supposed to be very small.

Essential and natural boundary conditions for Equation (1) are $\mathbf{u} = \mathbf{g}$ on $\Gamma_{\mathbf{g}}$ and $\mathbf{n} \cdot \left(-p\, \mathbf{I_d} + \frac{\nu_m}{\nu_f \sqrt{Gr}} \nabla \mathbf{u} \right) = \mathbf{h}$ on $\Gamma_{\mathbf{h}}$, where $\Gamma_{\mathbf{g}}$ and $\Gamma_{\mathbf{h}}$ are complementary subsets of the domain boundary Γ. Functions $\mathbf{g}$ and $\mathbf{h}$ are given, and $\mathbf{n}$ is the unit outward normal vector of Γ. A divergence-free velocity field $\mathbf{u}_0(\mathbf{x})$ is the initial condition for the velocity and $c_i(\mathbf{x}, 0)$ describing grain size composition and concentration of the suspended sediment in the begining of the current have to be prescribed for the transport equation. For equation (3), boundary conditions modeling the transport of particles into and out the flow domain are:

$$\begin{aligned} c &= c_n \text{ on } \Gamma_n^{c_i} \\ u_S \mathbf{e}^g \; c - \left(\frac{1}{Sc\sqrt{Gr}} \right) \nabla c) \cdot \mathbf{n} &= 0 \;\; \text{on } \Gamma_h^c \\ \frac{\partial c}{\partial t} - u_S \nabla c \cdot \mathbf{n} &= 0 \;\; \text{on } \Gamma_{bottom} \end{aligned}$$

with $\Gamma = \Gamma_n^c \cup \Gamma_h^c \cup \Gamma_{bottom}$ and $\Gamma_n^c \cap \Gamma_h^c \cap \Gamma_{bottom} = \emptyset$.

The former, a Dirichlet condition, describes the quantity of sediment entering in the flow domain. The second and third boundary conditions are enforced to reproduce physical mechanisms of particle motion through the remaining boundary, either by diffusion or advection. Sedimentation is allowed at the bottom on Γ_{bottom}. This last condition implies in loss of sediment but does not take into account any modification of the bottom geometry by deposition. Moreover, no particle resuspension mechanism, allowing particles to go back to the flow after hitting bottom, like erosion, is included. No significant amount of resuspension is expected for the flow conditions analyzed here, [6]. Therefore, at the bottom, the boundary condition is nothing but the net flux of sediment mass deposited by the current. Moreover, for each spatial point $\mathbf{x}$ on Γ_{bottom}, the contribution to the layer thickness resulting from the deposition

is given by integrating the particles fluxes till the time t resulting in surfaces defined over the bottom as:

$$D(\mathbf{x}, t) = \int_0^t u_S \; c(\mathbf{x}, t) \; d\tau \tag{6}$$

The resulting deposit thickness is obtained at each time t, the total height corresponding to the deposition on a specific point at the bottom is D_T. The final spatial maps computed at the end of the current ($t = t_\infty$), $D(\mathbf{x}, \infty)$, are considered in the present study of high interested, inasmuch they characterize the deposition patterns which can be used to infer a geological model of the basin, [7]. Those maps contain both thickness and composition of the deposits. At this point, it is important to recognize that the genesis of the final geologic formation occurs along a substantial period resulting from different events. In this sense, the above model is supposed to reproduce a single event. However, to obtain the final form, we have to consider a sequence of simulations in which each event deposits, and might erode, stacking sediment mass over the previous ones.

2.2 Phenomenological modeling: closure equations

The interdependence of the motion of the two components of the mixture, fluid, and sediments, is expressed in the above balance equations through a buoyancy term. The buoyancy term is proportional to several factors. The total sediment concentration at each spatial point acting on the fluid, the deposition mechanism embedded in the bottom boundary condition, the convective velocity in the transport equation, and, the particular focus here, a phenomenological relation to describe the effect of the sediment concentration on the viscosity. The modeling of this modified rheological behavior introduces a closure equation to the mathematical problem. Here we adopt, despite the variety of possibilities found in the literature [8], the model of [9],

$$\nu_m(c) = \nu_0 \Big(1 - \frac{c}{c_m}\Big)^{-2.5 c_m} \tag{7}$$

where c_m is the maximum volumetric concentration. This particular model has been used in [10] to help in the understanding of turbulence modulation in nondilute sediment transport. The above nonlinear phenomenological model is supposed to reproduce the rheological response of the mixture with a limited degree of accuracy, employed to pursue a compromise between computational costs and fidelity to reality. More sophisticated models, like those based on the two-fluid approach [10], are supposed to be more

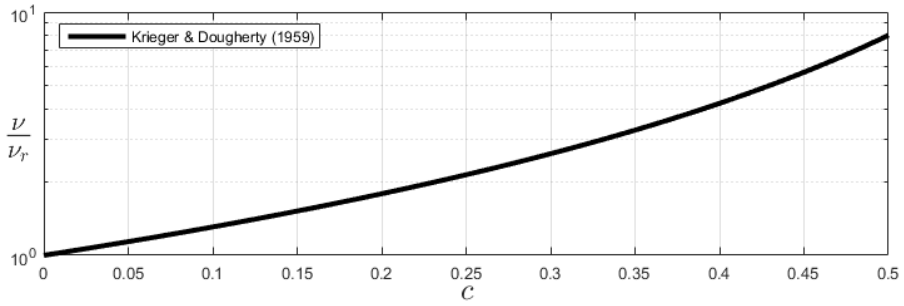

Figure 1. Nonlinear Krieger & Dougherty viscosity law from [8]

accurate, but the simulations would, typically, lead to more intense computations as well. Therefore, it is crucial to estimate the impact of potential pitfalls of those models in the final predictions. As example [11] presents an analysis of how the dynamics of turbidity currents react to empirical relations describing mass exchange with the surroundings and [12] carries out a validation of turbulent closure models for particle-laden flows. Figure 1 unveils that the phenomenological model built upon those tests display same trends of growth but also bear substantial differences regarding the viscosity values predicted for a given concentration, especially for medium and high concentrations. We propose here trying to improve our RB-VMS formulation with closure models to be embedded with the aim to analyze the impact on the results and reproduce the physics observed for sediment-water mixtures in standard rheological experiments [13].

3 Finite element formulation and turbulence subgrid modeling

The solver for the sediment transport coupled problem employed here relies on a weak formulation based on the Residual Based Variational Multiscale Method (RBVMS) introduced within the context of Finite Element Stabilized Methods. RBVMS have been used with success in the simulation of turbulent flows [14] , [15], [16], [17], [18], [19] and [20], free-surface flows [21] and multi-transport [22] and [23], two fundamental aspects of the present problem. Indeed, the finite element formulation employed here is a direct extension of the one proposed in [20] for polydisperse currents. The interested reader will find all details about the formulation, with a particular focus on the role of the subgrid modeling in the turbulent transport of the sediments in [20]. The governing equations approximated by RBVMS relies on a scales splitting of the physical variables combined with variational projections [20]. This splitting involving the large scales (those explicitly captured by the numerical grid) and the fine scales (subgrid scales). This splitting of scales is to be inserted in a standard weak formulation built upon Equations (1) to (3). Assuming as in [20] a simple algebraic model for the fine scales. Substituting the above expressions in the weak formulation for the coarse scales, we arrive at the final finite element formulation. It can be shown that RBVMS stabilizes the numerical solution for convection-dominated flows and also allows equal-order interpolation for velocity and pressure. Furthermore, the final formulation is now understood ([24], [25]) to lead to a Large Eddy Simulation (LES) framework, in which the fine scales model provides a subgrid model for turbulence. The turbulence structures within the turbidity currents, as the computational simulations to be presented later in this paper, involving recirculation and separation of the flow have a great impact on the final depositional pattern. In this respect, assuming that $\mathcal{V}$ denotes the trial function space for the velocity-pressure-concentration triple $\{\mathbf{u}, p, c\}$ and $\mathcal{W}$ the space of test functions for the momentum, continuity and sediment transport equations, denoted by $\{\mathbf{w}, q, \upsilon\}$, the weak form consist in find $\{\mathbf{u}, p, c\} \in \mathcal{V}$ such that $\forall\{\mathbf{w}, q, \upsilon\} \in \mathcal{W}$,

3.1 Computational Implementation and Solution Procedure

The RBVMS formulation presented in this work is implemented in the EdgeCFD software, which is an incompressible flow solver able to treat free-surface flow problems by a Volume-of-Fluid approach [21]. EdgeCFD is a parallel Fortran90 finite element code consisting of an outer time integration loop of two staggered-coupled systems of equations. Most of the computational cost comes from the **u**-p coupled solution of the incompressible flow equations while the cheapest part is due to the transport equation.

Pseudocode for coupled Navier–Stokes and Transport equations in EdgeCFD

```
1:  while t_o < t_f do
2:      while i < i_max do
3:          Solve Navier-Stokes equations
4:          Nonlinear method: Inexact-Newton Krylov
5:          Linear method: Preconditioned GMRES(m)
6:      end while
7:      while i < i_max do
8:          Solve Transport equations
9:          Nonlinear method: Predictor-Multicorrector
10:         Linear method: Preconditioned GMRES(m)
11:     end while
12:     if PID controller activated then
13:         compute time step Δt
14:     end if
15:     t = t + Δt
16: end while
```

EdgeCFD also supports the SUPG/PSPG formulation plus LSIC stabilization for the incompressible Navier-Stokes equations and the SUPG formulation with discontinuity–capturing for scalar transport [26] and [27]. EdgeCFD uses to treat turbulence by a Smagorinsky model [26]. This code uses a time integration predictor-multi-corrector algorithm with adaptive time stepping by a Proportional-Integral-Derivative (PID) controller (further details available in [28]).

Within the flow solution loop, the multi-correction steps correspond to the Inexact-Newton Krylov method with backtracking as described in [29]. In this approach, the nonlinear solver adapts the tolerance according to the evolution of the solution residuum. EdgeCFD iterative driver is the Generalized Minimal

Residual Method (GMRES) since the equation systems stemming from the incompressible flow and transport are non-symmetric.A nodal block diagonal preconditioner is employed for the flow and a simple diagonal preconditioner for the transport equations. Most of the computational effort spent in the solution phase is devoted to matrix-vector products. To compute such operations more efficiently, we use an edge-based data structure as detailed in [29]. The computations are performed in parallel using a distributed memory paradigm through the message passing interface library (MPI), using point-to-point communication [30]. The parallel partitions are generated by the Metis library [31] while the information regarding the edges of the computational grid is obtained from the EdgePack library as described in [32]. EdgePack also reorders nodes, edges, and elements to improve data locality, exploiting the memory hierarchy of current processors efficiently. Integrals in EdgeCFD are computed using closed–form relations derived in volume coordinates or using a one-point (centroid) integration rule. Thus, all coefficients in the element matrices and residue are explicitly coded. Therefore, if we evaluate $\mathbf{u} = \mathbf{u}_h + \mathbf{u}'$ and the stabilization parameters τ_M, τ_C and τ_t using values of the previous multi–correction, in a linearization scheme similar to the iteration-update of Tezduyar and Osawa [33] and Tezduyar [34], the RBVMS implementation in EdgeCFD for simulating particle-laden flows becomes straightforward. Moreover, in doing this, the only code modification required is computing τ_M and τ_t at the tetrahedra integration points. This evaluation is indeed straightforward for linear tetrahedra, requiring a few extra floating point operations and no additional memory but a few temporary variables. EdgeCFD is also able to solve fluid-structure interaction (FSI) problems within the Arbitrary Lagrangian Eulerian (ALE) formulation, which is useful to describe bed morphodynamics [35].

4 Computational Results

In this section, we showed the assessment of the RBVMS formulation as the capacity of the phenomenological viscosity law to enhance the predictions of the turbidity currents, to do this we break down the analysis into two examples. We analyse density currents over the flat and wavy bottom covered with 3D elements. Both cases take into consideration physical scenarios inspired in typical experimental setups. The computational procedure to modeling the sedimentation processes was explained in the previous section, carried through and simulated numerically with EdgeCFD. We will investigate the role played by phenomenological laws and bottom topography, both by changing the flow dynamics and by the effects on sediment deposition. The example to be analyzed deals with a channel configuration where a sediment stream is sustainedly injected by a window. This problem was studied from laboratory experiments and numerical simulations, [36] [37]. The difference between the densities of the heavy and the light fluid is set to less than 3% to match with the Boussinesq hypothesis. The initial condition, there is a domain filled with ambient fluid and a sediment fluid to be injected by a window with normalized concentration equal to 1.

4.1 Channel setups with flat and wavy floor

The computational setup, sketched in Figure **??**, shown the initial configuration, $t = 0$ where the mixture of sediments and is initially in the lock area and the concentration of sediments and deposition for at $t = 20$ after mixing with the clear ambient water in the channel. The channel dimensions' are $L_x = 12$, $L_y = 4$, $L_z = 2$, where the volume is fulfilled with ambient fluid (lighter) and the sediments (heavier fluid) injected through a inlet window with $h = 0.25$ height, .No-slip boundary condition was applied at the bottom and wall faces of the thank, in the top face, we specify an open flux boundary condition. The simulation last 20 non-dimensional time units and we consider for Reynolds number, $Re = 5,000$. The domains was discretized by $1.5M$ tetrahedra with $.7M$ nodes. Those values, combined with the settling velocities and initial concentrations defined previously, lead to high Grashoff numbers which meets laboratory standards, but it does not correspond to typically values of turbidity currents in nature. The mixture is injected with a concentration reference $C_0 = 0.01$.

The Grashoff number reached allows us to see the formation of turbulent structures that interact with the sediments and are responsible for the deposition patterns showed in Figure **??**.This figure illustrates the bottom complex pattern driven by the turbulent flow pattern resulting of total deposition. Figure **??** shows font views of the concentration at $x = 5$ and $x = 10$ at the end of the discharge ($t = 30$). On the left the results for the $Re = 5k$ and on the right for $Re = 10k$. The concentration variations compare the solutions with constant viscosity with the ones where the viscosity is given by the Krieger and Dougherty nonlinear law. It is evident the effect of the nonlinear viscosity over the dynamics of the

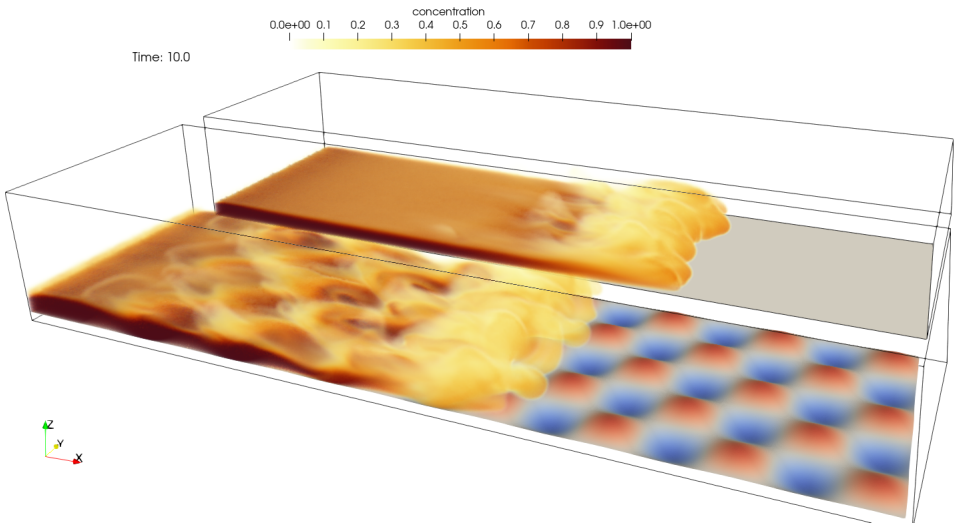

Figure 2. Channel setups with flat and wavy bottom

current, particularly near the bottom of the channel.

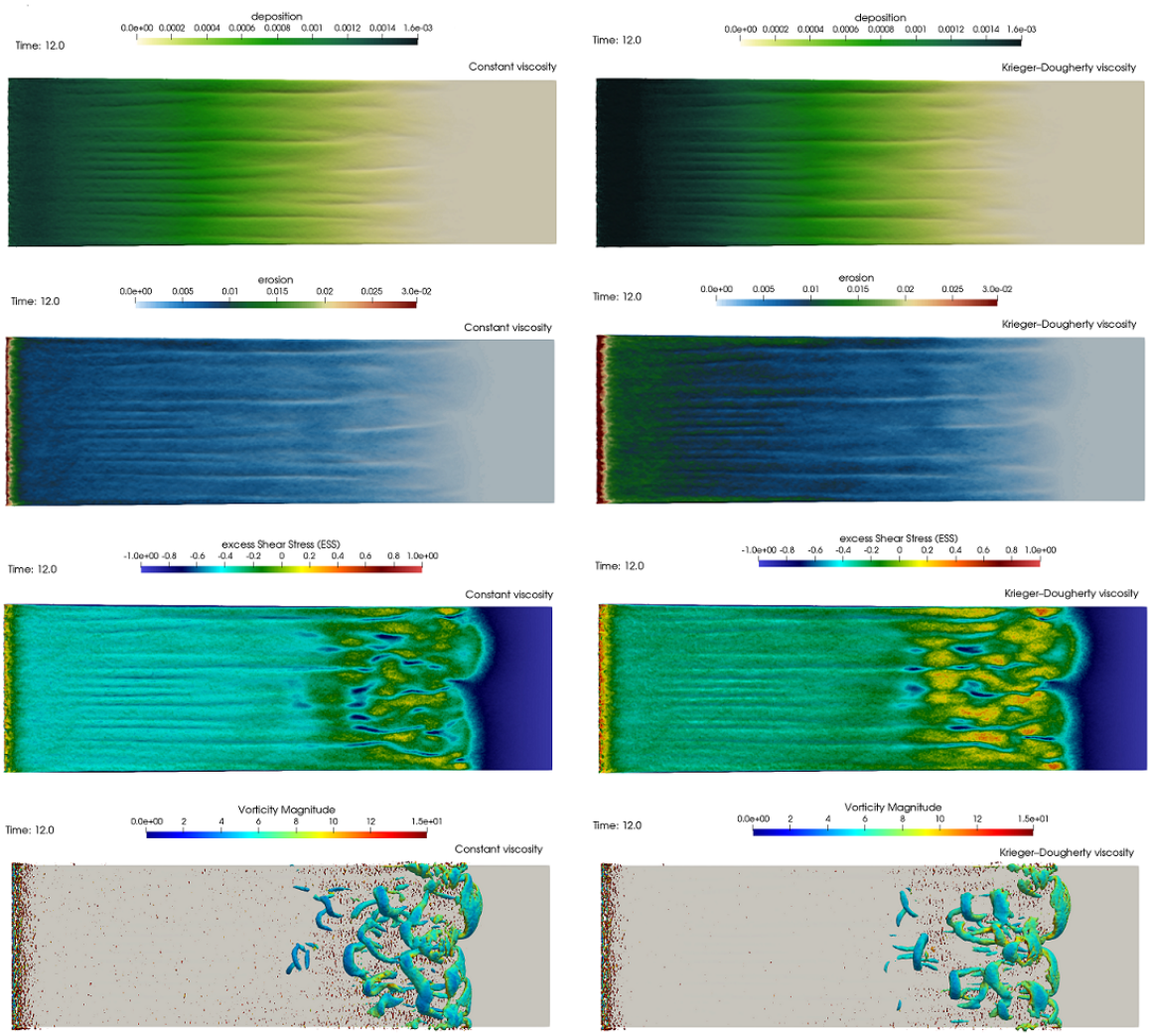

Figure 3. Flat bottom, from up to down, deposition, erosion of sediments, excess of shear stress and iso-contours of Q-criterium colored by vorticity for constant viscosity (left) and Krieger Dougherty viscocity law (right) at t= 12

Figure 3 portrays a top view of the deposition, erosion, excess shear stresses and iso-contours of Q-criterium colored by vorticity for standard simulation with constant viscosity and considering the Krieger Dougherty viscosity law for the setup with flat bottom. It is important to note, that although (flow and sediment transport) is in a particular snapshot is enough to see the complex spatial characteristics. Over the time period simulated, the flow is highly three dimensional with lobe and cleft instabilities, behavior more accentuated in the case of constant viscosity. The excess shear stresses and observe the higher values, mainly where the current is driven by the inlet (sustained current). Note also the region away from the inlet, where turbulence can be more relevant for the resuspension mechanism. We can notice remarkable differences between both solutions again. These results make clear the importance of phenomenological model on the dynamics of the turbidity currents.

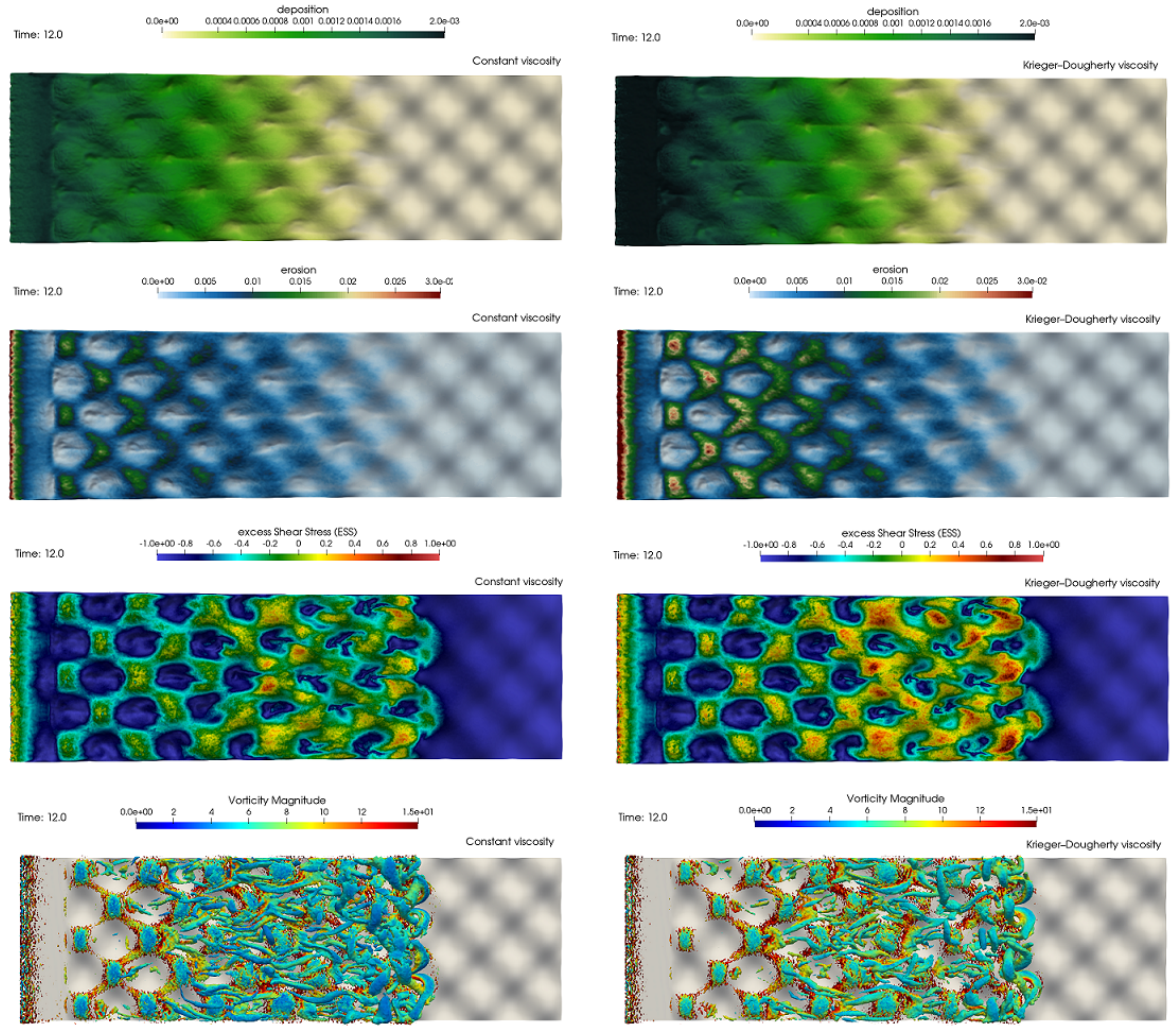

Figure 4. Wavy bottom, from up to down, deposition, erosion of sediments, excess of shear stress and iso-contours of Q-criterium colored by vorticity for constant viscosity (left) and Krieger Dougherty viscocity law (right) at t= 12

Figure 4 shows the particle-laden gravity currents over wavy bottom floor where effect of the height of the waves on the flow physics is analysed. Like a previous figure, same quantities re presented. The presence of waves at the bottom increases substantially to turbulence in the evolution of the current, this is evident trough the results of the Q-criterium. The increment of viscosity by the concentration-dependent viscosity, given by Krieger and Dougherty law reduce this turbulence like observed in flats results and increment the deposition at the bottom of the wells. We can notice again, remarkable differences between both solutions that makes clear the importance of those phenomenological models on the dynamics of the turbidity currents. a typical solution, that is, on top, the sediment concentration and below, the correspondent sediment deposit. Note the complex deposit pattern driven by the turbulent flow. The wavy bottom revealing complex interactions of the turbidity current with the irregular topography.

4.2 Conclusions and Future Work

Here, a numerical formulation for simulating particle-laden gravity currents is presented using the framework of RBVMS, in which the coupling between the fine-scale velocity and the residual of density concentration equation is represented. The simulation of sustained particle-laden gravity currents in a channel over flat an wavy bottom floor is presented considering viscosity dependant concentration in the formulation. The analyses are performed over a flat and wavy bottom and compared the results considering the effects of viscosity. It was found the flow behavior is noticeably changed, as the wave height bottom. The the current front speed affect the particle settling by the presence of bottom and by the viscosity too. The simulations over flat and wavy bottoms are performed and compared the results considering the Krieger Dougherty viscosity. It was found the flow behavior is noticeably changed, as the wave height increases. The wave height bottom decrease the current front speed and slow down the particle settling but in the other hand the viscosity augmented te erosion.

This work shown that this kind of analyses are useful to enhance the understanding, qualitatively and quantitatively of sedimentary depositional systems resulting from turbidity currents takeing into consideration the physics of the flow, sediment transport, and deposition mechanisms interacting with irregulars bottoms.

5 Acknowledgments

The authors would like to thank the support of PETROBRAS Technological Program on Basin Modeling in the name of its general coordinator, Dr. Marco Moraes. Partial support is also provided by MCT/CNPq and FAPERJ. Computer resources were provided by the High Performance Computer Center, COPPE/UFRJ.

References

[1] J. E. Simpson. *Gravity Currents: In the Environment and the Laboratory*, volume 1. Cambridge University Press, 1997.

[2] E. Meiburg and B. Kneller. Turbidity currents and their deposits. *Annual Review of Fluid Mechanics*, vol. 42, n. 1, pp. 135–156, 2010.

[3] A. J.R.L. *Principles of Physical Sedimentology*, volume 1. The Blackburn Press, 1985.

[4] M. Nasr-Azadani, B. Hall, and E. Meiburg. Polydisperse turbidity currents propagating over complex topography: Comparison of experimental and depth-resolved simulation results. *Computers and Geosciences*, vol. 53, pp. 141–153. Modeling for Environmental Change, 2013.

[5] M. I. Cantero, S. Balachandar, M. H. García, and D. Bock. Turbulent structures in planar gravity currents and their influence on the flow dynamics. *Journal of Geophysical Research: Oceans*, vol. 113, n. C8, pp. n/a–n/a, 2008.

[6] F. Necker, H. C., K. L., and E. Meiburg. Mixing and dissipation in particle-driven gravity currents. *Journal of Fluid Mechanics*, vol. 53, 2005.

[7] J. R. L. Herbert E. Huppert. Roger T. Bonnecaze. Patterns of sedimentation from polydispersed turbidity currents. *Proceedings: Mathematical, Physical and Engineering Sciences*, vol. 452, n. 1953, pp. 2247–2261, 1996.

[8] P. Widera, P. E. Toorman, and P. C. Lacor. Large eddy simulation of sediment transport in open-channel flow. *Journal of Hydraulic Research*, vol. 47, n. 3, pp. 291–298, 2009.

[9] I. M. Krieger and T. J. Dougherty. A mechanism for non-newtonian flow in suspensions of rigid spheres. *Transactions of The Society of Rheology*, vol. 3, n. 1, pp. 137–152, 1959.

[10] X. Yu, T.-J. Hsu, and S. Balachandar. A spectral-like turbulence-resolving scheme for fine sediment transport in the bottom boundary layer. *Computers and Geosciences*, vol. 61, pp. 11 – 22, 2013.

[11] M. M. Traer, A. Fildani, T. McHargue, and G. E. Hilley. Simulating depth-averaged, one-dimensional turbidity current dynamics using natural topographies. *Journal of Geophysical Research: Earth Surface*, vol. 120, n. 8, pp. 1485–1500, 2015.

[12] E. A. Toorman, ed. *Validation of macroscopic modelling of particle-laden turbulent flows*, volume 1. 6th Belgian National Congress on Theoretical and Applied Mechanics, 2003.

[13] M. Pavlik. *The dependence of suspension viscosity on particle size, shear rate, and solvent viscosity.* PhD thesis, De Paul Universtiy, Illinois, 2009.

[14] Y. Bazilevs, V. Calo, J. Cottrell, T. Hughes, A. Reali, and G. Scovazzi. Variational multiscale residual-based turbulence modeling for large eddy simulation of incompressible flows. *Computer Methods in Applied Mechanics and Engineering*, vol. 197, pp. 173 – 201, 2007.
[15] R. Codina, J. M. González-Ondina, G. Díaz-Hernández, and J. Principe. Finite element approximation of the modified boussinesq equations using a stabilized formulation. *International Journal for Numerical Methods in Fluids*, vol. 57, n. 9, pp. 1249–1268, 2008.
[16] R. Codina, S. Badia, J. Baiges, and J. Principe. *Variational Multiscale Methods in Computational Fluid Dynamics*, chapter 1, pp. 1–28. American Cancer Society, 2017.
[17] N. Ahmed, T. Chacón Rebollo, V. John, and S. Rubino. A review of variational multiscale methods for the simulation of turbulent incompressible flows. *Archives of Computational Methods in Engineering*, vol. 24, n. 1, pp. 115–164, 2017.
[18] I. Akkerman, Y. Bazilevs, V. M. Calo, T. J. R. Hughes, and S. Hulshoff. The role of continuity in residual-based variational multiscale modeling of turbulence. *Computational Mechanics*, vol. 41, n. 3, pp. 371–378, 2008.
[19] U. Rasthofer and V. Gravemeier. Recent developments in variational multiscale methods for large-eddy simulation of turbulent flow. *Archives of Computational Methods in Engineering*, pp. 1–44, 2017.
[20] G. M. Guerra, S. Zio, J. J. Camata, F. A. Rochinha, R. N. Elias, P. L. Paraizo, and A. L. Coutinho. Numerical simulation of particle-laden flows by the residual-based variational multiscale method. *International Journal for Numerical Methods in Fluids*, vol. 73, n. 8, pp. 729–749, 2013.
[21] E. F. Lins, R. N. Elias, F. A. Rochinha, and A. L. G. A. Coutinho. Residual-based variational multiscale simulation of free surface flows. *Computational Mechanics*, vol. 46, n. 4, pp. 545–557, 2010a.
[22] A. Ehrl, G. Bauer, V. Gravemeier, and W. A. Wall. A computational approach for the simulation of natural convection in electrochemical cells. *Journal of Computational Physics*, vol. 235, pp. 764 – 785, 2013.
[23] G. Bauer, V. Gravemeier, and W. A. Wall. A stabilized finite element method for the numerical simulation of multi-ion transport in electrochemical systems. *Computer Methods in Applied Mechanics and Engineering*, pp. 199 – 210, 2012.
[24] J. Principe, R. Codina, and F. Henke. The dissipative structure of variational multiscale methods for incompressible flows. *Computer Methods in Applied Mechanics and Engineering*, vol. 199, pp. 791 – 801. Turbulence Modeling for Large Eddy Simulations, 2010.
[25] R. Calderer and A. Masud. Residual-based variational multiscale turbulence models for unstructured tetrahedral meshes. *Computer Methods in Applied Mechanics and Engineering*, vol. 254, pp. 238 – 253, 2013.
[26] R. N. Elias and A. L. G. A. Coutinho. Stabilized edge-based finite element simulation of free-surface flows. *International Journal for Numerical Methods in Fluids*, vol. 54, n. 6-8, pp. 965–993, 2007.
[27] R. N. Elias, P. L. B. Paraizo, and A. L. G. A. Coutinho. Stabilized edge-based finite element computation of gravity currents in lock-exchange configurations. *International Journal for Numerical Methods in Fluids*, vol. 57, pp. 1137–1152, 2008.
[28] A. M. P. Valli, G. F. Carey, and A. L. G. A. Coutinho. Control strategies for timestep selection in finite element simulation of incompressible flows and coupled reaction–convection–diffusion processes. *International Journal for Numerical Methods in Fluids*, vol. 47, n. 3, pp. 201–231, 2005.
[29] R. N. Elias, M. A. D. Martins, and A. L. G. A. Coutinho. *Parallel Edge-Based Inexact Newton Solution of Steady Incompressible 3D Navier-Stokes Equations*, chapter 1, pp. 1237–1245. Springer Berlin Heidelberg, Berlin, Heidelberg, 2005.
[30] E. F. Lins, R. N. Elias, F. A. Rochinha, and A. L. G. A. Coutinho. Residual-based variational multiscale simulation of free surface flows. *Computational Mechanics*, vol. 46, n. 4, pp. 545–557, 2010b.
[31] G. Karypis and V. Kumar. A fast and high quality multilevel scheme for partitioning irregular graphs. *SIAM J. Sci. Comput.*, vol. 20, n. 1, pp. 359–392, 1998.
[32] A. L. G. A. Coutinho, M. A. D. Martins, R. M. Sydenstricker, and R. N. Elias. Performance comparison of data-reordering algorithms for sparse matrix–vector multiplication in edge-based unstructured grid computations. *International Journal for Numerical Methods in Engineering*, vol. 66, n. 3, pp. 431–460, 2006.
[33] T. E. Tezduyar and Y. Osawa. Finite element stabilization parameters computed from element matrices and vectors. *Computer Methods in Applied Mechanics and Engineering*, vol. 190, pp. 411 – 430, 2000.
[34] T. E. Tezduyar. Computation of moving boundaries and interfaces and stabilization parameters. *International Journal for Numerical Methods in Fluids*, vol. 43, n. 5, pp. 555–575, 2003.
[35] J. J. Camata, R. N. Elias, and A. L. G. A. Coutinho. Fem simulation of coupled flow and bed

morphodynamic interactions due to sediment transport phenomena. *JCST*, vol. 7, n. 2, pp. 306–321, 2013.
[36] K. Bhaganagar. Direct numerical simulation of lock-exchange density currents over the rough wall in slumping phase. *Journal of Hydraulic Research*, vol. 52, n. 3, pp. 386–398, 2014.
[37] S. Xu, N. Liu, and J. Yan. Residual-based variational multi-scale modeling for particle-laden gravity currents over flat and triangular wavy terrains. *Computers and Fluids*, vol. 188, pp. 114–124, 2019.